



Submitted to

32nd International Conference on High Energy Physics, ICHEP04, August 16, 2004, Beijing

Abstract: **12-0188**

Parallel Session **4,12**

www-h1.desy.de/h1/www/publications/conf/conf.List.html

Search for Events with Tau Leptons in ep Collisions at HERA

H1 Collaboration

Abstract

The production of tau leptons in ep collisions is studied with the H1 detector at HERA. The identification algorithm is based on the search for isolated charged tracks associated to narrow hadronic jets detected in the calorimeters, a typical signature of the one-prong hadronic tau decay. Using this identification procedure, a search for events with high P_T isolated tau leptons and missing transverse momentum is performed using a data sample collected with the H1 detector at HERA, corresponding to an integrated luminosity of 108 pb^{-1} . This search complements the previously published observation of isolated electrons and muons in events with missing transverse momentum. In addition, a search for events with tau lepton pairs produced in elastic photon-photon collisions is performed.

1 Introduction

The HERA collaborations H1 and ZEUS have previously reported the observation of events with isolated high energy electrons and muons in events with significant missing transverse momentum, P_T^{miss} . [1–4]. The dominant Standard Model (SM) contribution to this topology is the production of real W bosons with subsequent leptonic decay. Such events can also be a signature of new phenomena beyond the Standard Model, for example the production of single top quarks via Flavour Changing Neutral Currents (FCNC) [5, 6].

In this paper we present a search for events with tau leptons using the H1 detector. The analysis uses the data collected between 1996 and 2000, corresponding to an integrated luminosity of 108 pb^{-1} . The hadronic decays of tau leptons are searched for in events with significant missing transverse momentum. A search for events containing tau-pairs produced in photon-photon collisions is also presented here.

Another search for events with isolated tau leptons and missing transverse momentum at HERA was recently published by the ZEUS Collaboration [7].

This paper is organised as follows. Section 2 describes the physics processes contributing to signal and background in the search of events with high P_T tau leptons. Section 3 describes the H1 detector and experimental conditions relevant to the analysis. Section 4 describes the search for events with tau leptons and missing transverse momentum. Section 5 presents a search for events with tau lepton pairs, followed by conclusions.

2 Processes and their Monte Carlo Simulation

The processes within the Standard Model that contribute to the searched topology are briefly outlined in this section.

The following SM processes produce events containing genuine isolated tau leptons and genuine missing transverse momentum in the final state:

- *Production of W bosons:*

In the Standard Model, the main source of isolated tau leptons with high transverse momenta is the production of W bosons with subsequent decay $W \rightarrow \tau\nu_\tau$. The production of the electroweak vector bosons W^\pm as well as Z^0 is modelled using the EPVEC [8] generator. The NLO QCD corrections to W production [9] are taken into account by weighting the events as a function of the rapidity and transverse momentum of the W boson [10].

- *Lepton pair production:*

The contribution from tau pair production is dominated by two-photon processes where at least one of the produced taus decays hadronically. For this process, the genuine missing transverse momentum is low and should be aligned with the tau pair direction in the transverse plane for high P_T tau pair production. The production of muons can also contribute as a background to the searched topology if one of the muons fakes a tau signature. The contribution from lepton pair production is calculated using the GRAPE [11] generator.

Other processes contribute to the selected sample through misidentification or mismeasurement. A fake tau lepton, fake missing transverse momentum or both can be reconstructed and may lead to the topology of interest. The following processes are considered:

- *Charged current deep inelastic scattering:*
The main background to the tau and P_T^{miss} topology is the charged current (CC) deep inelastic scattering process, which contains genuine large missing transverse momentum due to the scattered neutrino. In these events, a hadronic jet can have low multiplicity and mimic the tau signature. This background contribution is calculated using the DJANGO [12] program.
- *Neutral current processes:*
Events containing no genuine missing transverse momentum may contribute to the searched topology via an energy measurement fluctuation which may induce significant P_T^{miss} . This is the case for the neutral current (NC) and multi-jet photoproduction (γp) processes. In NC events the scattered electron can also mimic a narrow hadronic jet, while for the γp events one of the jets in the final state may have low multiplicity and fake the tau candidate. The background contribution from NC deep inelastic scattering is modelled using the RAPGAP [13] generator. Multi-jet events with photon virtualities $Q^2 < 4 \text{ GeV}^2$ are modelled with the PYTHIA Monte Carlo generator [14]. Both generators rely on first order QCD matrix elements and use leading-log parton showers and string fragmentation [15]. Both light and heavy quark flavours are generated. The GRV LO (GRV-G LO) parton densities in the proton (photon) are used [16].

Finally, as a prototype for physics beyond the Standard Model, the anomalous production of single top quarks at HERA is considered:

- *Anomalous single top production:*
The single top production via flavour changing neutral currents at HERA fulfills the signal selection, if the decay of the top quark in a bottom quark and a W boson is followed by the decay of the W into $\tau \nu_\tau$. Genuine missing transverse momentum is generated by the presence of neutrinos in the event. This process is expected to have a high P_T^X due to the presence of the b-quark jet from top decay. It is simulated using the generator ANOTOP [6] and is used for qualitative comparisons with the results of the present analysis.

All generated events are passed through the full GEANT [17] based simulation of the H1 apparatus and are reconstructed using the same program chain as for the data.

3 Experimental Conditions

At HERA electrons or positrons with an energy E_e of 27.6 GeV collide with protons at an energy of 920 GeV, giving a centre-of-mass energy of $\sqrt{s} = 319 \text{ GeV}$. Up to 1997 the proton

energy was 820 GeV, giving $\sqrt{s} = 301$ GeV. The analysis is based on HERA I data set recorded by the H1 experiment between 1996 and 2000, which corresponds to an integrated luminosity of 108 pb^{-1} .

A detailed description of the H1 detector can be found in [18]. Only the components essential for this analysis are described here. The right handed Cartesian coordinate system used in the following has its origin at the nominal primary ep interaction vertex. The proton direction defines the z axis. The polar angle θ and transverse momenta P_T are defined with respect to this axis.

The inner tracking system contains the central ($25^\circ < \theta < 155^\circ$) and forward ($7^\circ < \theta < 25^\circ$) drift chambers. It is used to determine the position of the interaction vertex and to measure the trajectories of charged particles. Particle transverse momenta are determined from the curvature of the trajectories in a solenoidal magnetic field of 1.15 Tesla.

Hadronic final state particles as well as electrons and photons are absorbed in the highly segmented liquid argon (LAr) calorimeter [19] ($4^\circ < \theta < 154^\circ$), which is 5 to 8 hadronic interaction lengths deep depending on the polar angle. The LAr also includes an electromagnetic section which is 20 to 30 radiation lengths deep. Electromagnetic shower energies are measured with a precision of $\sigma(E)/E = 12\%/\sqrt{E/\text{GeV}} \oplus 1\%$, hadronic shower energies with $\sigma(E)/E = 50\%/\sqrt{E/\text{GeV}} \oplus 2\%$, as determined in test beam measurements [20]. In the backward region ($153^\circ < \theta < 178^\circ$), the LAr is complemented by a lead-scintillating fibre spaghetti calorimeter (SPACAL) [21]. In the forward region ($0.6^\circ < \theta < 3.5^\circ$) the LAr is complemented by a sandwich calorimeter constructed from copper plates and silicon counters (PLUG) [22].

The calorimeter is contained within a superconducting coil and an iron return yoke, instrumented with streamer tubes, which is used as a muon detector and covers the range $4^\circ < \theta < 171^\circ$. Tracks of penetrating particles, such as muons, are reconstructed from their hit pattern in the streamer tubes and are detected with an efficiency of above 90%. The instrumented iron also serves as a backing calorimeter to measure the energies of hadrons that are not fully absorbed in the LAr.

The events studied in this analysis are triggered by requiring large missing transverse momentum measured in the calorimeter. At the trigger level the missing transverse momentum is identified using the vector sum of LAr “trigger towers”, which are groups of trigger regions with a projective geometry pointing to the nominal interaction vertex. The trigger efficiency is 50% (85%) for events with a missing transverse momentum above 12 GeV (25 GeV).

4 Search for Events with Missing Transverse Momentum and Isolated Tau Leptons

This search aims to complement the previous observation of events with electrons or muons and significant P_T^{miss} . Due to the difficult tau lepton identification, more powerful background suppression is required.

The identification of events with missing transverse momentum is based on the following observables that quantify the momentum imbalance in the event:

- P_T^{calo} , the net transverse momentum measured from all energy deposits recorded in the calorimeters.
- P_T^{miss} , the total missing transverse momentum reconstructed from all observed particles (electrons, muons and hadrons). P_T^{miss} differs most from P_T^{calo} in the case of events with muons, since they deposit little energy in the calorimeter.
- $E - P_z = \sum_i E_i(1 - \cos \theta_i)$, where E_i and θ_i denote the energy and polar angle of each particle in the event detected in the main detector. For an event where only momentum in the proton direction is undetected, $E - P_z = 2E_e = 55$ GeV ($E_e = 27.5$ GeV is the electron beam energy). This quantity gives a measure of the longitudinal momentum balance.

The hadronic final state (HFS) is measured by combining calorimeter energy deposits with low momentum tracks. Identified isolated electrons or muons are excluded from the hadronic final state. The calibration of the hadronic energy scale is made by comparing the transverse momentum of the precisely measured scattered electron to that of the HFS in a large NC event sample. Particles from the reconstructed HFS are combined into jets using an inclusive k_T algorithm with a minimum P_T of 4 GeV.

The tau candidate forms a narrow hadronic jet associated to one isolated charged track measured in the inner tracker. The present analysis restricts the search for hadronic tau decays to the “one-prong” decays, which make up 50% of the total tau decay width. The size of the hadronic jet is estimated using the jet radius R_{jet} , defined as the energy weighted average distance in the $\eta - \phi$ plane between the jet axis and the hadrons making up the jet:

$$R_{jet} = \frac{1}{E_{jet}} \sum_i E_i \sqrt{\Delta\eta(jet, i)^2 + \Delta\phi(jet, i)^2}$$

where the sum runs over all hadrons that belong to the candidate hadronic jet. The isolation of the tau candidate is measured by the distance in $\eta - \phi$ plane to the closest hadronic jet (D_{jet}) or to the closest track (D_{track}). The remaining hadronic system after excluding the tau jet candidate, is denoted by X hereafter.

The selection of events with isolated tau candidates and missing transverse momentum is performed in three steps:

- P_T^{miss} **preselection** (table 1).
The candidate events are selected if the calorimetric transverse momentum is greater than 12 GeV. The missing transverse momentum, P_T^{miss} is also required to be above 12 GeV and the longitudinal momentum imbalance $E - P_z < 45$ GeV. In order to further suppress the NC and γp processes, a topological cut is applied on the acoplanarity between the transverse momentum measured in the central calorimeter and that measured by the forward PLUG calorimeter $\Delta\phi(Calo, PLUG)$ as a function of P_T^{calo} , as described in table 1. The cut is harsher at lower P_T^{calo} where the background is higher, while at $P_T^{\text{calo}} > 25$ GeV the cut has no effect. Additionally, at least one jet with $P_T > 7$ GeV is required. The system X is defined at this stage as the hadronic final state excluding the highest p_T jet.

After these cuts, 4142 events are selected, in good agreement with the SM prediction of 4100 ± 851 . Figure 1 presents the global event variables $E - P_z$, P_T^{calo} and the P_T of the highest P_T jet. Figure 2 presents the jet radius of this jet and the transverse momentum P_T^X of the remaining hadronic system. At this stage, for all distributions, the data are in good agreement with the Monte Carlo simulation.

- $\tau + P_T^{miss}$ **preselection** (table 2).

In the remaining data sample, events containing tau candidates are selected. The tau candidate selection is based on the typical signature of the hadronic one prong tau decay: one charged track associated to a narrow ("pencil-like") hadronic deposit in the calorimeter. The tau lepton candidates are selected from the reconstructed hadronic jets. The candidate hadronic jet is required to have a $P_T > 7$ GeV and to be in the polar angle range $20^\circ < \theta < 120^\circ$. The jet is required to contain only one charged track and to be isolated from other jets or charged tracks: $D_{jet} > 1$ and $D_{track} > 1$.

After this selection step, 26 events are selected in the data, well in agreement with the expectation of 24.2 ± 4.4 . The distributions of the jet radius R_{jet} of the selected jet and of the remaining hadronic transverse momentum P_T^X at this stage are presented in figure 3. Good agreement is observed between the data and the Monte Carlo simulation.

- $\tau + P_T^{miss}$ **final selection** (table 3).

Narrow "pencil-like" jets are selected by the requirement $R_{jet} < 0.12$. The acoplanarity $\Delta\phi(jet, X)$ between the tau candidate momentum and the momentum of the remaining measured particles in the event is required to be below 170° . In order to further suppress the mainly low P_T background, further cuts $P_T^{calo} > 20$ GeV and $P_{track} > 5$ GeV are applied.

After the final selection, five events are observed in the data sample compared to a SM expectation of 5.8 ± 1.3 . The P_T^X spectrum after the final selection is shown in figure 4. The data events are in the very low P_T^X region. In the region at large hadronic momentum $P_T^X > 25$ GeV no events are observed. Table 4 summarizes the results of the search.

This preliminary analysis completes the picture of the searches for events with isolated leptons and missing transverse momentum at HERA. The status after HERA I data taking is summarised in table 5. While H1 reports events with electrons and muons in the high P_T^X region in excess to the SM prediction, ZEUS observes good agreement with the Standard Model. In turn, ZEUS observes two tau events at large P_T^X for 0.20 ± 0.05 expected. The new H1 preliminary search for $\tau + P_T^{miss}$ events presented here reveals no candidate at large P_T^X . In the tau channel, the H1 analysis has a W detection efficiency which is roughly two times that of the ZEUS analysis in the high- P_T^X region. The background suppression of the ZEUS analysis is roughly two times stronger than that of the H1 analysis in the same region.

5 Observation of Tau Pairs in Elastic $\gamma\gamma$ -processes.

As a supplementary investigation of the ability of the H1 detector to detect tau leptons, a preliminary search for elastic tau-pair production in ep collisions is performed. Events with semi-leptonic tau decays are selected by requiring one identified electron or muon and one hadronic tau candidate (1-prong or 3-prong) with $P_T > 2$ GeV. The hadronic tau signature is verified by a neural network algorithm, based mainly on hadronic cluster shape and trained differently for one- or three-prong candidates. In order to select elastic events, events with additional energy deposits or tracks that cannot be interpreted as being due to the scattered electron are rejected.

With this selection, 15 events are observed with opposite charges of the two tau leptons, compatible with an expectation of 17.6 ± 3.9 events, dominated by the tau-pair process. A selected data event is presented in figure 6. In the event sample with like-sign charges, dominated by elastic NC scattering, 1 event is observed for an expectation of 1.9 ± 1.2 .

The distribution of the visible transverse momentum of the hadronically decaying tau lepton, reconstructed by the hadronic cluster, is shown in figure 5. The results of the preliminary search for elastic tau-pair production are in agreement with the expectation and demonstrate the ability of the H1 detector to detect tau leptons.

6 Conclusions

The search for isolated tau leptons presented here completes the analyses of isolated leptons and missing P_T performed by the experiments H1 and ZEUS experiments using the data collected during HERA I running period. In a data sample corresponding to an integrated luminosity of 108 pb^{-1} , five data candidates are selected in the final analysis for an expectation of 5.8 ± 1.4 . No selected data event has a hadronic system with large transverse momentum $P_T^X > 25$ GeV, a region where 0.5 events are expected. A preliminary search for tau pairs produced in elastic photon-photon collisions has also been performed in the semileptonic decay mode. After a neural network based identification of hadronic tau decay, 15 events with opposite charges of the two tau leptons are selected in the data for an expectation of 17.6, dominated by the tau-pair production process.

References

- [1] T. Ahmed *et al.* [H1 Collaboration], DESY preprint 94-248 (1994).
- [2] C. Adloff *et al.* [H1 Collaboration], Eur. Phys. J. C **5**, 575 (1998) [hep-ex/9806009].
- [3] J. Breitweg *et al.* [ZEUS Collaboration], Phys. Lett. B **471** (2000) 411 [hep-ex/9907023].
- [4] V. Andreev *et al.* [H1 Collaboration], Phys. Lett. B **561** (2003) 241 [hep-ex/0301030].
- [5] S. Chekanov *et al.* [ZEUS Collaboration], Phys. Lett. B **559** (2003) 153 [hep-ex/0302010].

- [6] A. Aktas *et al.* [H1 Collaboration], Eur. Phys. J. C **33** (2004) 9 [arXiv:hep-ex/0310032].
- [7] S. Chekanov *et al.* [ZEUS Collaboration] Phys. Lett. B **583** (2004) 41
- [8] U. Baur, J. A. M. Vermaseren and D. Zeppenfeld, Nucl. Phys. B **375** (1992) 3.
- [9] K.-P. Diener, C. Schwanenberger and M. Spira, Eur. Phys. J. C **25** (2002) 405 [hep-ph/0203269];
P. Nason, R. Rückl and M. Spira, J. Phys. G **25** (1999) 1434 [hep-ph/9902296];
M. Spira, Proc. of the Workshop “Monte Carlo Generators for HERA Physics” (1991), Eds. A. T. Doyle, G. Grindhammer, G. Ingelman, H. Jung, p. 623 [hep-ph/9905469].
- [10] K.-P. Diener, C. Schwanenberger and M. Spira, hep-ex/0302040.
- [11] T. Abe, Comput. Phys. Commun. **136** (2001) 126 [hep-ph/0012029].
- [12] DJANGO 2.1; G.A. Schuler and H. Spiesberger, Proc. of the Workshop “Physics at HERA” (1991), Eds. W. Buchmüller and G. Ingelman, Vol. 3, p. 1419.
- [13] H. Jung, Comput. Phys. Commun. **86** (1995) 147; RAPGAP program manual (1998) unpublished [<http://www-h1.desy.de/~jung/RAPGAP.html>].
- [14] PYTHIA 5.7; T. Sjöstrand, CERN-TH-6488 (1992), Comp. Phys. Comm. **82** (1994) 74.
- [15] JETSET 7.4; T. Sjöstrand, Lund Univ. preprint LU-TP-95-20 (1995) 321pp;
idem, CERN preprint TH-7112-93 (1994) 305pp.
- [16] M. Glück, E. Reya and A. Vogt, Phys. Rev. D **45** (1992) 3986;
idem, Phys. Rev. D **46** (1992) 1973.
- [17] GEANT3; R. Brun *et al.*, CERN-DD/EE/84-1.
ANOTOP
- [18] I. Abt *et al.* [H1 Collaboration], Nucl. Instrum. Meth. A **386** (1997) 310 and 348.
- [19] B. Andrieu *et al.* [H1 Calorimeter Group], Nucl. Instrum. Meth. A **336** (1993) 460.
- [20] B. Andrieu *et al.* [H1 Calorimeter Group], Nucl. Instrum. Meth. A **344** (1994) 492;
B. Andrieu *et al.* [H1 Calorimeter Group], Nucl. Instrum. Meth. A **350** (1994) 57;
B. Andrieu *et al.* [H1 Calorimeter Group], Nucl. Instrum. Meth. A **336** (1993) 499.
- [21] R. D. Appuhn *et al.* [H1 SPACAL Group], Nucl. Instrum. Meth. A **386** (1997) 397.
- [22] W. Hildesheim *et al.*, H1 Internal Note, **H1-IN-372** (08/1994).

P_T^{miss} Preselection	
P_T^{calo}	$> 12 \text{ GeV}$
P_T^{miss}	$> 12 \text{ GeV}$
$\Delta\phi(Calo, \text{PLUG})$	$< 150^\circ + 30^\circ \cdot \left(\frac{P_T^{calo}-12}{13}\right)$
$\Sigma(E - P_z)$	$< 45 \text{ GeV}$
N_{jets}	≥ 0
P_T^{jet}	$> 7 \text{ GeV}$

Table 1: The preselection of events with missing transverse momentum: P_T^{calo} is the total calorimetric transverse momentum, P_T^{miss} is the total transverse momentum of all reconstructed particles, $\Delta\phi(Calo, \text{PLUG})$ is the acoplanarity between the momentum measured in the main calorimeter and the momentum measured in the forward PLUG calorimeter, $\Sigma(E - P_z)$ sums the $E - P_z$ contributions of all measured particles and is 55.2 GeV for events with fully measured final state. At least one jet is required with a transverse momentum above 7 GeV.

$\tau + P_T^{miss}$ Preselection	
P_T^{miss} Preselection	(see table 1)
P_T^{jet}	$> 7 \text{ GeV}$
θ^{jet}	from 20° to 120°
N_{tracks}	$= 1$
P_T^{track}	$> 2 \text{ GeV}$
$D_{jet,track}$	> 1.0

Table 2: The preselection of events with significant missing transverse momentum and a single track jet, corresponding to a tau candidate. The jet polar angle θ^{jet} is required to be in the central region and to contain exactly one charged track with a transverse momentum above 2 GeV. The jet is required to be isolated by asking the minimum distance in the $\eta - \varphi$ plane to other tracks or jets in the event to be above 1.

$\tau + P_T^{miss}$ Final Selection	
P_T^{miss} Preselection	(see table 1)
P_T^{calo}	> 20 GeV
P_T^{jet}	> 7 GeV
θ^{jet}	from 20° to 120°
N_{tracks}	$= 1$
P_T^{track}	> 5 GeV
$R_{e,\mu,jets}^{\eta\varphi}$	> 1.0
$\Delta\phi(jet, X)$	$< 170^\circ$
R^{jet}	< 0.12 GeV

Table 3: Final selection of events with isolated tau candidates and missing transverse momentum. Narrow calorimetric deposits are identified using the variable R^{jet} (jet size), defined by $R_{jet} = \sum_i \frac{E_i \Delta^i(\varphi, \eta)}{E^{jet}}$ (i runs over all particles in the jet, E_i is the particle energy and $\Delta^i(\varphi, \eta)$ the distance in $\eta - \varphi$ plane to the jet axis). The hadronic final state excluding the tau candidate jet is denoted by X . A significant acoplanarity requirement $\Delta\phi(jet, X) < 170^\circ$ ensures further background rejection.

H1 Preliminary

H1 Data 96-00 108 pb ⁻¹	Data	All SM Processes	SM W	Single top Efficiency * BR
Full Sample	5	5.81 ± 1.36	0.87 ± 0.15	0.52 %
$P_T^X > 25$ GeV	0	0.53 ± 0.10	0.26 ± 0.05	0.49 %
$P_T^X > 40$ GeV	0	0.22 ± 0.05	0.12 ± 0.03	0.42 %

Table 4: Observed and predicted number of events in the 1996-2000 dataset after the final selection. Also shown is the the product of the efficiency and the branching fraction for the anomalous single top production detected in the channel $t \rightarrow bW(\rightarrow \tau\nu_\tau)$ (the present analysis is only sensitive to the one-prong hadronic tau decays)

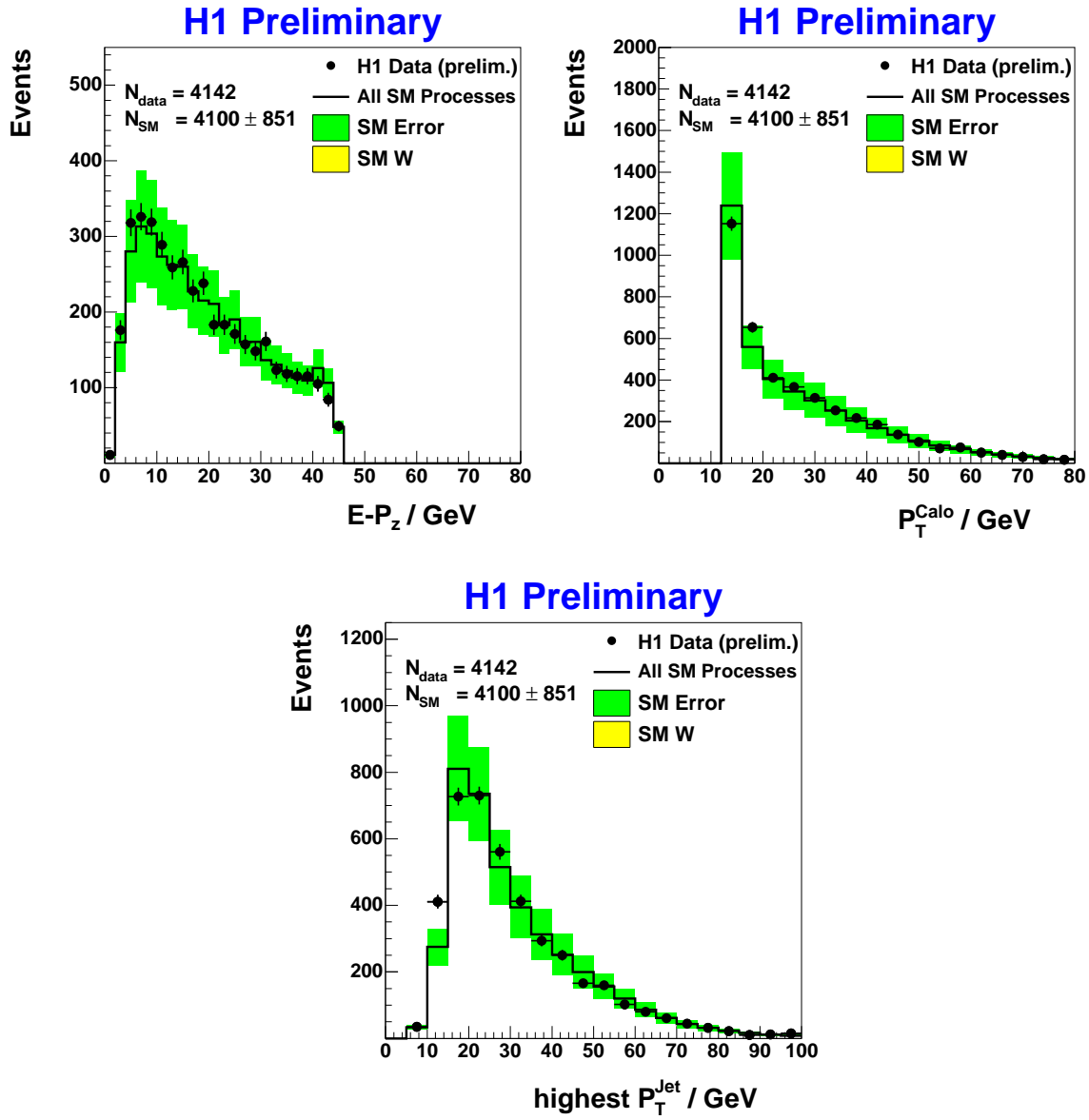


Figure 1: The distributions of $\Sigma(E - P_z)$, P_T^{calo} and the highest P_T^{jet} in the data compared to the Monte Carlo simulation for the P_T^{miss} event preselection described in table 1. The SM W contribution is still negligible at this level.

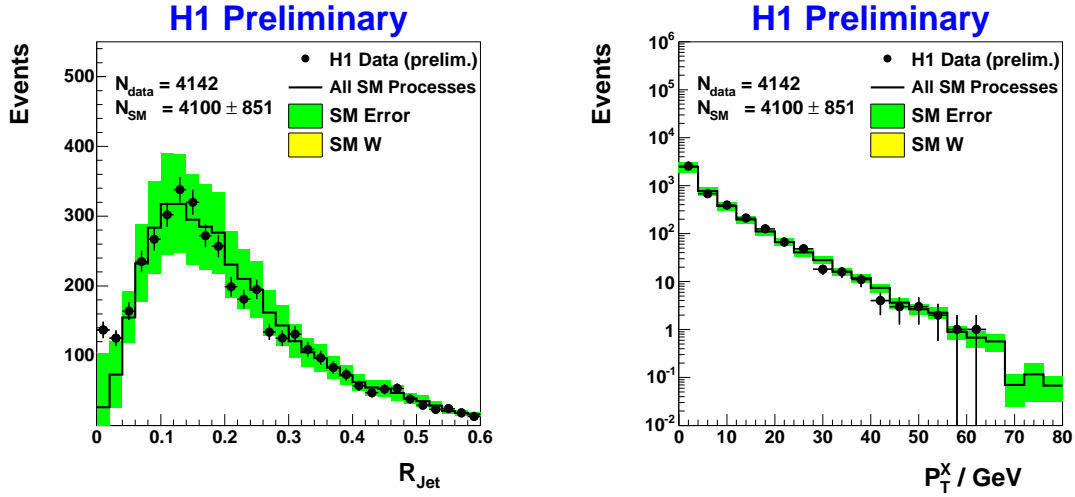


Figure 2: The distributions of R^{jet} and P_T^X in the data compared with the Monte Carlo simulation for the P_T^{miss} event preselection described in table 1. The SM W contribution is still negligible at this level.

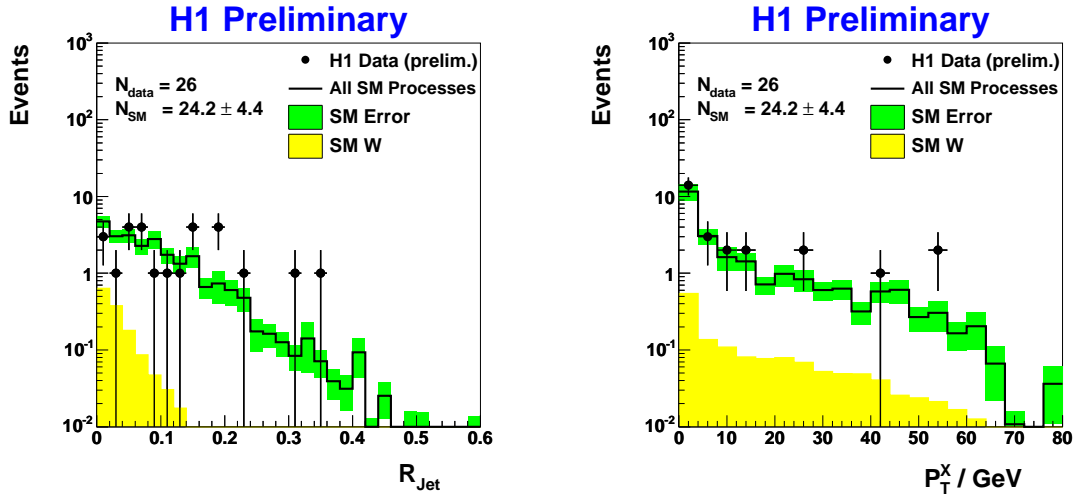


Figure 3: The distributions of R^{jet} and P_T^X in the data compared with the Monte Carlo simulation for the $\tau + P_T^{\text{miss}}$ event preselection described in table 2. Note that the jet radius R^{jet} of jets selected in the Standard Model W Monte Carlo are narrow, as expected from tau jets. A cut $R^{\text{jet}} < 0.12$ is applied later in the final selection.

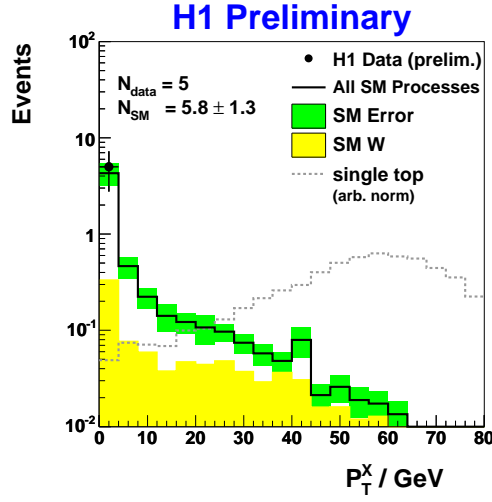


Figure 4: The distribution of the hadronic transverse momentum P_T^X in the data compared with the Monte Carlo simulation for the $\tau + P_T^{miss}$ final selection described in table 3. No events are observed in the high P_T^X region, where events for the template signal process single top production are expected.

1994-2000 $e^\pm p$		Electron obs./exp. (W^\pm contrib.)	Muon obs./exp. (W^\pm contrib.)	Tau (H1:108 pb^{-1}) obs./exp. (W^\pm contrib.)
H1 118.4 pb^{-1}	Full Sample	11 / 11.54 \pm 1.50 (71%)	8 / 2.94 \pm 0.50 (86%)	5 / 5.81 \pm 1.36 (15%)
	$P_T^X > 25$ GeV	5 / 1.76 \pm 0.30 (82%)	6 / 1.68 \pm 0.30 (88%)	0 / 0.53 \pm 0.10 (49%)
	$P_T^X > 40$ GeV	3 / 0.66 \pm 0.13 (80%)	3 / 0.64 \pm 0.14 (92%)	0 / 0.22 \pm 0.05 (54%)
ZEUS 130.2 pb^{-1}	Full Sample	24 / 20.6 $^{+1.7}_{-4.6}$ (17%)	12 / 11.9 $^{+0.6}_{-0.7}$ (16%)	3 / 0.40 $^{+0.12}_{-0.13}$ (49%)
	$P_T^X > 25$ GeV	2 / 2.90 $^{+0.59}_{-0.32}$ (45%)	5 / 2.75 $^{+0.21}_{-0.21}$ (50%)	2 / 0.20 $^{+0.05}_{-0.05}$ (49%)
	$P_T^X > 40$ GeV	0 / 0.94 $^{+0.11}_{-0.10}$ (61%)	0 / 0.95 $^{+0.14}_{-0.10}$ (61%)	1 / 0.07 $^{+0.02}_{-0.02}$ (71%)

Table 5: Summary of the results of searches for events with isolated leptons, missing transverse momentum and large P_T^X at HERA. The number of observed events is compared to the SM prediction. The W^\pm component is given in parentheses in percent. The statistical and systematic uncertainties added in quadrature are also indicated.

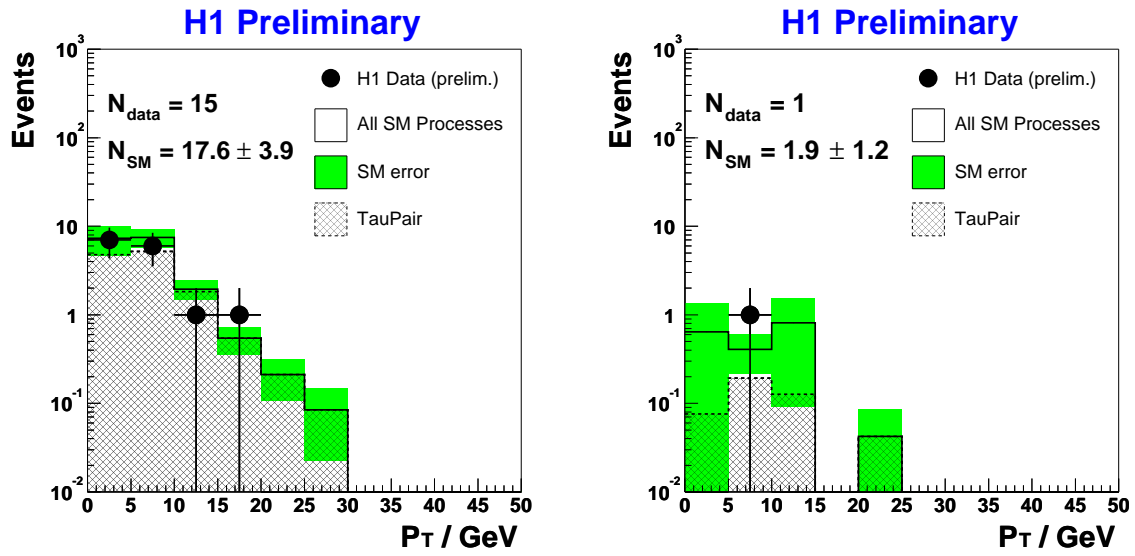


Figure 5: Control Plots of the visible transverse momentum distributions of the hadronically decaying tau lepton; on the left for opposite charges of the two decaying tau candidates, on the right for equally charged tau candidates. In $\gamma\gamma \rightarrow \tau^+\tau^-$ processes only candidates of opposite charge are expected.

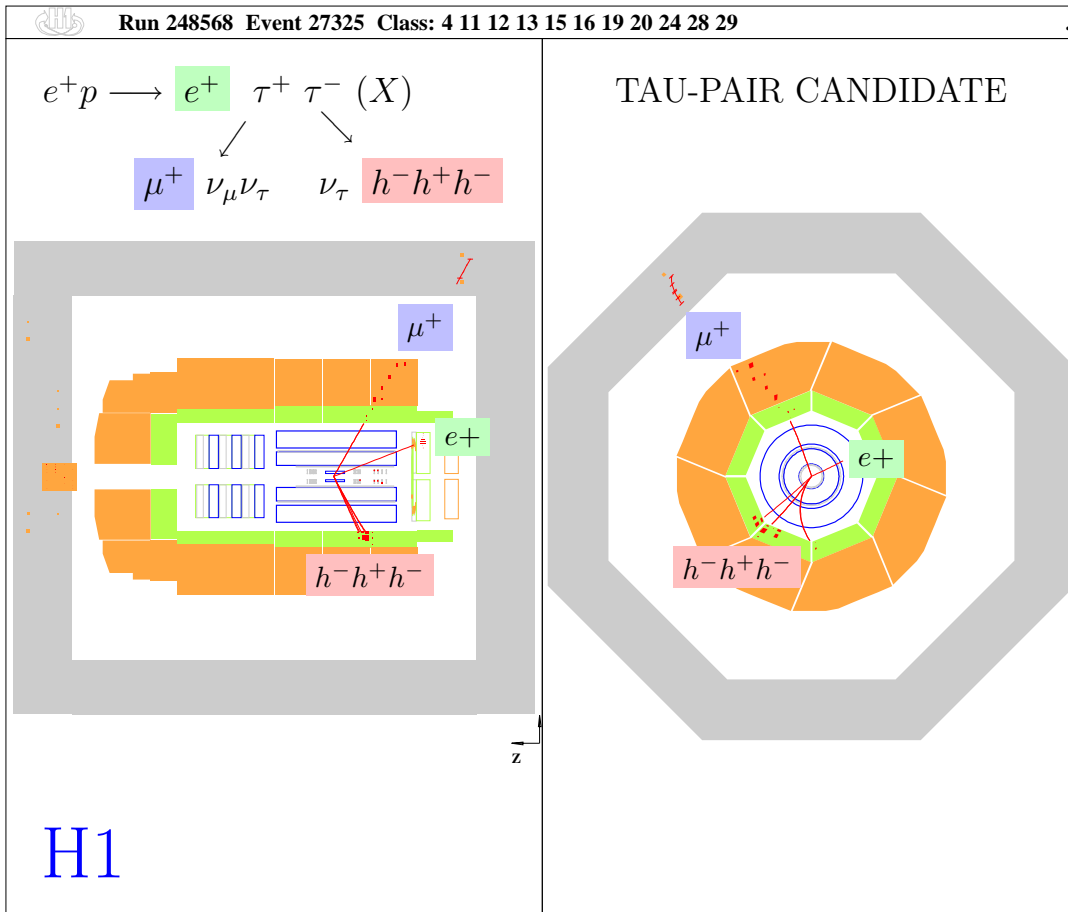


Figure 6: Tau-pair candidate event with one tau lepton decaying leptonically to a muon, and the other tau lepton decaying to three charged hadrons (3-prong topology). The scattered positron is also detected in the backward calorimeter.